Proceedings of the 7th International Symposium on Cavitation
CAV2009 - Paper No. 42
August 17-22, 2009, Ann Arbor, Michigan, USA

Investigation on numerical schemes in the simulation of barotropic cavitating flows

Marco Bilanceri
Dip. Ingegneria Aerospaziale
via Caruso, 8 - 56122 Pisa
University of Pisa - Italy
email: m.bilanceri@ing.unipi.it

François Beux
Dip. Ingegneria Aerospaziale
via Caruso, 8 - 56122 Pisa
University of Pisa - Italy
email: f.beux@alta-space.com

Maria Vittoria Salvetti
Dip. Ingegneria Aerospaziale
via Caruso, 8 - 56122 Pisa
University of Pisa - Italy
email: mv.salvetti@ing.unipi.it

ABSTRACT

A numerical methodology for the simulation of cavitating flows is considered. A homogeneous-flow cavitation model, accounting for thermal effects and active nuclei concentration, is considered, which leads to a barotropic state law. The continuity and momentum equations for compressible inviscid flows are discretized through a finite-volume approach, applicable to unstructured grids. The numerical fluxes are computed by shock-capturing schemes and ad-hoc preconditioning is used to avoid accuracy problems in the low-Mach regime. Second-order accuracy in space is obtained through MUSCL reconstruction. Time advancing is carried out by an implicit linearized scheme. Two different numerical fluxes are investigated here, viz. the Roe and the Rusanov schemes. For the Rusanov flux two different time linearizations are proposed; in the first one the upwind part of the flux function is frozen in time, while in the second one its time variation is taken into account, although in an approximated manner. The different schemes and the different linearizations are appraised for the quasi 1D-flow in a nozzle through comparison against exact solutions and for the flow around a hydrofoil mounted in a wind tunnel through comparison against experimental data. Non-cavitating and cavitating conditions are simulated. It is shown that, for cavitating conditions, the Rusanov scheme together with the more complete time linearization allows time steps much larger than for the Roe scheme to be used. Finally, the results obtained with this scheme are in good agreement with the exact solutions or the experimental data for all the considered test cases.

INTRODUCTION

The present work is part of a research aimed at developing a tool for numerical simulation of 3D compressible flows satisfying a generic barotropic equation of state. In particular, we are interested in simulating cavitating flows through the barotropic homogeneous flow model proposed in [1]. In previous works, see e.g. [2, 3], a linearized implicit, second-order accurate, numerical method for the simulation of compressible barotropic flows on unstructured grids was developed. This numerical scheme is based on a finite-volume spatial discretization, through the Roe numerical flux function [4] and a MUSCL reconstruction technique [5] to obtain second-order accuracy. A time-consistent preconditioning is introduced to deal with the low Mach number regime. The linearized implicit time-advancing is associated to a defect-correction technique to obtain a second-order accurate (both in time and space) formulation at a limited computational cost. The set-up numerical tool has been validated through a rather extensive set of numerical experiments and the obtained results were in good agreement with experimental data and analytical solutions. However, when cavitation occurs, the stability properties of the scheme deteriorate dramatically and only very small time steps are allowed. This clearly increases the computational costs and, thus, makes difficult to afford the simulation of complex cavitating flows, as occur in many aerospace and industrial applications. To overcome this problem a different numerical flux function, namely the Rusanov one (see [6, 7]), is considered in this work. The Rusanov numerical flux function is known to have excellent robustness properties and thus it seems to be a good candidate to eliminate, or at least reduce, the instabilities

connected with the cavitation. The same steps used to develop the numerical tool based on the Roe numerical flux function are herein followed for the Rusanov case. First, it has been verified that preconditioning is needed also for the Rusanov scheme to deal with the low-Mach regime and a suitable preconditioning is defined. Moreover, the linearized implicit time advancing technique is defined. Note that for the Rusanov scheme, also thanks to its simplicity, two different linearizations are proposed: the first one is a classical linearization, in which the upwind part of the flux is considered frozen, as it is usually done in the literature for the family of upwind schemes to which the Roe and Rusanov ones belong (see, e.g., [8] or [9]). Conversely, in the second linearization the time variation of this upwind part is taken into account, although in an approximate manner. This may be important when the speed of sound has a stiff change in magnitude, as typically occurs for homogeneous-flow models in presence of cavitation. Finally, the same ingredients developed to achieve second-order accuracy for the Roe scheme, i.e. MUSCL reconstruction and defect correction, are also applied to the Rusanov numerical flux.

A first series of 1D simulations for the steady flow in a convergent-divergent nozzle have been performed in order to compare the different schemes and numerical formulations. As a first-order scheme is generally more stable than the corresponding second-order and we are interested in robustness, in this first set of simulations we only use the first-order version of the considered schemes.

Then, the developed numerical methodology and the different schemes are applied to the simulation of the inviscid flow around a hydrofoil mounted in a wind tunnel [10] both in cavitating and non-cavitating conditions. The accuracy of the results is appraised by comparison against experimental data [11]. The robustness and efficiency of the different considered schemes is also investigated.

As a final remark, we are aware that a known drawback of the Rusanov numerical flux function is the introduction of a too large numerical dissipation in presence of contact discontinuities and, thus, this scheme is not well suited for viscous computations. However, in the literature there are modifications of the Rusanov scheme which reduce this problem without loosing in robustness, as for instance the HLLC [7] or HLLE+ flux functions [12]. In the spirit of the HLLE+ scheme, we have developed an original modification of the Rusanov flux function, aimed at improving the behavior in presence of contact discontinuities. However, in this paper only inviscid flow simulations are presented and has been checked that, as expected, this modification has not significant effects for inviscid flows. Thus, this modified Rusanov scheme is not presented here for sake of brevity.

PHYSICAL MODELING

State and governing equations

A weakly-compressible liquid at constant temperature T_L is considered as working fluid. The liquid density ρ is allowed to locally fall below the saturation limit $\rho_{Lsat} = \rho_{Lsat}(T_L)$ thus originating cavitation phenomena. A regime-dependent (wetted/cavitating) constitutive relation is therefore adopted.
As for the wetted regime ($\rho \geq \rho_{Lsat}$), a barotropic model of the form

$$p = p_{sat} + \frac{1}{\beta_{sL}} \ln\left(\frac{\rho}{\rho_{Lsat}}\right) \tag{1}$$

is adopted, $p_{sat} = p_{sat}(T_L)$ and $\beta_{sL} = \beta_{sL}(T_L)$ being the saturation pressure and the liquid isentropic compressibility, respectively. As for the cavitating regime ($\rho < \rho_{Lsat}$), a homogeneous-flow model explicitly accounting for thermal cavitation effects and for the concentration of the active cavitation nuclei in the pure liquid has been adopted [1]. In this model, the evaporation/condensation phenomena between the two phases take place within a layer surrounding the cavity surface, within which the temperature is assumed to be constant. Hence, the variation of the liquid entropy, as produced by the interfacial heat transfer, is opposite to the one of the cavities and therefore the entropy of the mixture does not change. The entropy conservation permits to derive a differential barotropic relation for the cavitating mixture as well

$$\frac{p}{\rho}\frac{d\rho}{dp} = (1-\alpha)\left[(1-\varepsilon_L)\frac{p}{\rho_{Lsat}a_{Lsat}^2} + \varepsilon_L g^\star \left(\frac{p_c}{p}\right)^\eta\right] + \frac{\alpha}{\gamma_V} \tag{2}$$

where $g^\star$, η, γ_V and p_c are liquid parameters, a_{Lsat} is the liquid sound speed at saturation, $\alpha = 1-\rho/\rho_{Lsat}$ and $\varepsilon_L = \varepsilon_L(\alpha,\zeta)$ is a given function (see [1] for its physical interpretation and for more details). The resulting unified barotropic state law for the liquid and for the cavitating mixture only depends on the two parameters T_L and ζ. For instance, for water at $T_L = 293.16K$, the other parameters involved in (1) and (2) are: $p_{sat} = 2806.82$ Pa, $\rho_{Lsat} = 997.29$ kg/m^3, $\beta_{sL} = 5\,10^{-10}$ Pa^{-1}, $g^* = 1.67$, $\eta = 0.73$, $\gamma_V = 1.28$, $p_c = 2.21\,10^7$ Pa and $a_{Lsat} = 1415$ m/s [13].

Note that despite the model simplifications leading to a unified barotropic state law, the transition between wetted and cavitating regimes is extremely abrupt. Indeed, the sound speed falls from values of order 10^3 m/s in the pure liquid down to values of order 0.1 or 1 m/s in the mixture. The corresponding Mach number variation renders this state law very stiff from a numerical viewpoint.

The 3D Euler equations for an inviscid fluid are considered as governing equations. Nevertheless, by virtue of the barotropic state law, the energy balance is decoupled from the mass and momentum balances; hence, it is possible to consider the following

reduced set of governing equations

$$\frac{\partial W}{\partial t} + \mathrm{div}(\vec{\mathcal{F}}(W)) = 0 \tag{3}$$

where $W = (\rho, \rho u, \rho v, \rho w)^T$ is the conservative variables vector and $\vec{\mathcal{F}}(W) = (F_x, F_y, F_z)^T$ represents the classical flux functions for mass and momentum balances.

The 1D case is used as a first step for the definition of the different numerical approaches, which are then extended and implemented in the 3D case. Thus, the following 1D flow system is also considered:

$$\frac{\partial W}{\partial t} + \frac{\partial F(W)}{\partial x} = 0 \tag{4}$$

where $W = (\rho, \rho u, \rho\xi)^T$ and $F(W) = \left(\rho u, \rho u^2 + p, \rho u \xi\right)^T$ in which ξ denotes a passive scalar. As for the 3D case, the energy equation does not need to be included since the partial derivatives system (4) is closed through a barotropic equation of state.

For the development of the numerical methods a generic barotropic equation of state is considered:

$$p = p(\rho) \tag{5}$$

The derivative $dp/d\rho$ is assumed to be strictly positive (a classical thermodynamic stability requirement for common fluids) and can be regarded to as the square of the fluid sound speed $a(\rho)$. The equations (1) and (2) for the cavitating case are a particular instance of (5).

NUMERICAL FORMULATION

The spatial discretization of the governing equations is based on a finite-volume formulation on unstructured tetrahedral grids and time advancing is carried out through an implicit linearized algorithm. For sake of simplicity, the different numerical ingredients are presented in details in the 1D case; the generalization to 3D is then briefly discussed.

Spatial discretization

The finite-volume spatial discretization of Eqs. (4) leads to the following semi-discrete problem:

$$\delta x_i \frac{\mathrm{d}W_i}{\mathrm{d}t} + \Phi_{i(i+1)} - \Phi_{(i-1)i} = 0 \tag{6}$$

where δx_i is the width of the finite-volume cell i and Φ_{ij} is a numerical flux function between the i-th cell and the j-th one. A family of classical first-order upwind schemes can be defined by the following expression of the numerical flux function:

$$\Phi_{ij} = \Phi_{ij,c} + \Phi_{ij,u} \tag{7}$$

in which the centered part $\Phi_{ij,c}$ and the upwind one $\Phi_{ij,u}$ are defined as:

$$\Phi_{ij,c} = \frac{F(W_i) + F(W_j)}{2}, \quad \Phi_{ij,u} = -\frac{1}{2} Q_{ij} (W_j - W_i) \tag{8}$$

The various schemes differ for the definition of the upwind term, and, more specifically, of the matrix Q_{ij}.

The Roe scheme One of the most popular choices for $\Phi_{i,j}$ is the Roe numerical flux function [4], defined by:

$$Q_{ij} = |\tilde{J}(W_i, W_j)| \tag{9}$$

The so-called Roe matrix $\tilde{J}$ is a diagonalizable matrix satisfying specific conditions [4] while $|\tilde{J}| = T\,|D|\,T^{-1}$ where T is the matrix of the eigenvectors associated with $\tilde{J}$ and $|D| = \mathrm{diag}(|\lambda_1|, \cdots, |\lambda_k|, \cdots, |\lambda_n|)$, λ_k being the k-th eigenvalue of $\tilde{J}$. Clearly, the Roe matrix, originally defined in [4] for the case of the Euler equations with an ideal-gas state law, depends on the specific hyperbolic problem under consideration. For a generic barotropic state equation (5) and the 1D hyperbolic system (4) the following Roe matrix has been derived in [3, 14]:

$$\tilde{J}_{ij} = \begin{pmatrix} 0 & 1 & 0 \\ \tilde{a}_{ij}^2 - \tilde{u}_{ij}^2 & 2\,\tilde{u}_{ij} & 0 \\ -\tilde{u}_{ij}\,\tilde{\xi}_{ij} & \tilde{\xi}_{ij} & \tilde{u}_{ij} \end{pmatrix} \tag{10}$$

in which $\tilde{u}_{ij}$ and $\tilde{\xi}_{ij}$ correspond to the well-known "Roe averages" for the states W_i and W_j of u and ξ respectively whereas $\tilde{a}_{ij}$, which can be identified with a Roe average for the sound speed, is defined as:

$$\tilde{a}_{ij} = \begin{cases} \sqrt{\dfrac{p(\rho_j) - p(\rho_i)}{\rho_j - \rho_i}} & \text{if } \rho_j \neq \rho_i \\ a(\rho_\star, p(\rho_\star)) & \text{if } \rho_i = \rho_j = \rho_\star \end{cases} \tag{11}$$

The Rusanov scheme Another common choice for $\Phi_{i,j}$ is the Rusanov scheme [6], which is defined by the choice of a diagonal matrix for Q_{ij}; more precisely:

$$Q_{ij} = \lambda_{ij} I$$

where I is the identity matrix and the parameter λ_{ij} is an upper bound for the fastest signal velocities [7]. This scheme can be viewed as a simple example of HLL Riemann solvers (see e.g. [7]). This class of robust approximate Riemann solvers are based on the construction of averaging intermediate states in the solution of the Riemann problem. The Rusanov scheme assumes only one intermediate wave state between two acoustic waves and λ_{ij} corresponds to the acoustic wavespeed estimate. Two of the most common choices are:

$$\lambda_{ij} = \max(|u_j| + a_j, |u_i| + a_i) \tag{12}$$

and the one based on the eigenvalues of the Roe matrix, that is in our case:

$$\lambda_{ij} = \max(|\tilde{u}_{ij} + \tilde{a}_{ij}|, |\tilde{u}_{ij} - \tilde{a}_{ij}|) \tag{13}$$

where $\tilde{u}_{ij}$ is the Roe average for u and $\tilde{a}_{ij}$ is defined by (11).

Preconditioning for low Mach number flows

For the cavitating flow problem, a large part of the flow is characterized by very low Mach numbers since we have to deal with a weakly-compressible liquid. Compressible solvers exhibit accuracy problems when dealing with nearly-incompressible flows [15]. In order to counteract this difficulty, some preconditioning must be applied.

A preconditioned Roe scheme A Turkel-like preconditioning has been proposed in [14, 16] for the Roe flux function associated with a barotropic equation of state using a similar formulation as proposed in [15] for a perfect-gas state law. This preconditioning is acting only on the upwind part of the numerical flux function; more precisely, (9) is substituted by:

$$Q_{ij} = P^{-1}(W_i, W_j)|P(W_i, W_j)\tilde{J}(W_i, W_j)|$$

where $P(W_i, W_j)$ is the preconditioning matrix.

It has been shown in [14,16] that, with an adequate choice of $P(W_i, W_j)$, the preconditioned semi-discrete solution recovers the same asymptotic behavior (with an expansion in power of a reference Mach number M) of the analytical one. This theoretical result has been also corroborated by numerical experiments which show that the preconditioned formulation does not present accuracy problems for low Mach number flows. We refer to [14, 16] for more details.

A preconditioned Rusanov scheme By carrying out the same asymptotic analysis as in [14, 16], it has been found that the Rusanov scheme also encounters accuracy problems in the low Mach number limit and, as a consequence, a preconditioning technique is needed to recover the correct behavior of the solution. In the spirit of [17], it is possible to work directly on the term of the matrix Q_{ij} without adding extra terms in the flux expression and, therefore, it is possible to consider the following "preconditioned matrix":

$$Q_{ij} = \lambda_{ij} \begin{pmatrix} \theta^{-1} & 0 & 0 \\ 0 & \theta & 0 \\ 0 & 0 & 1 \end{pmatrix} \tag{14}$$

where the parameter θ is defined as

$$\theta = \theta(M) = \begin{cases} 10^{-6} & \text{if } M \leq 10^{-6} \\ \min(M, 1) & \text{otherwise} \end{cases} \tag{15}$$

in which $M = \dfrac{|u|}{a}$, with u and a defined accordingly with the choice of λ_{ij}, i.e. if, for instance, $\lambda_{ij} = \tilde{u}_{ij} + \tilde{a}_{ij}$ then $u = \tilde{u}_{ij}$ and $a = \tilde{a}_{ij}$ and similarly for the other choices of λ_{ij}. With this simple preconditioning procedure, the correct asymptotic behavior of the analytical solution is recovered (see [18]) .

Extension to second-order accuracy in space The extension to second-order accuracy in space can be achieved by using a classical MUSCL technique [5], in which instead of $\Phi_{i,i+1} = \Phi(W_i, W_{i+1})$, the numerical flux $\Phi_{i+\frac{1}{2}} = \Phi(W^-_{i+\frac{1}{2}}, W^+_{i+\frac{1}{2}})$ is computed as a function of the extrapolated variable values at the cell interface $x_{i+\frac{1}{2}}$. The considered values $W^{\pm}_{i+\frac{1}{2}}$ are defined by piecewise linear reconstruction of the solution, and can be expressed as follows in a β-scheme form (see, e.g. [19]):

$$\begin{cases} W^-_{i+\frac{1}{2}} = W_i + \dfrac{h_{i+1}}{2}\left[(1-\beta)\dfrac{W_{i+1} - W_i}{h_{i+1}} + \beta\dfrac{W_i - W_{i-1}}{h_i}\right] \\ W^+_{i+\frac{1}{2}} = W_{i+1} - \dfrac{h_{i+1}}{2}\left[(1-\beta)\dfrac{W_{i+1} - W_i}{h_{i+1}} + \beta\dfrac{W_{i+2} - W_{i+1}}{h_{i+2}}\right] \end{cases}$$

where β is a given parameter. Note that this technique can equivalently be applied either to the Roe or to the Rusanov numerical flux.

Linearized implicit time advancing

A first-order accurate linearized implicit approach Let us consider an implicit backward Euler method applied to the semi-discrete problem (6):

$$\frac{\delta x_i}{\Delta^n t}\Delta^n W_i + \Delta^n \Phi_{i,i+1} - \Delta^n \Phi_{i-1,i} = -\left(\Phi^n_{i,i+1} - \Phi^n_{i-1,i}\right) \tag{16}$$

where $\Delta^n(\cdot) = (\cdot)^{n+1} - (\cdot)^n$. To avoid the solution of a nonlinear system at each time step, a linearization of $\Delta^n \Phi_{ij}$ is usually adopted. A way to obtain such a linearization is to find two matrices D_1 and D_2 such that

$$\Delta^n \Phi_{ij} \simeq D_1(W_i^n, W_j^n)\,\Delta^n W_i + D_2(W_i^n, W_j^n)\,\Delta^n W_j \qquad (17)$$

In this case (16) is reduced to the following block tridiagonal linear system:

$$B_{-1}^{i,n}\,\Delta^n W_{i-1} + B_0^{i,n}\,\Delta^n W_i + B_1^{i,n}\Delta^n W_{i+1} = -\left(\Phi_{i,i+1}^n - \Phi_{i-1,i}^n\right)$$

where:

$$\begin{cases} B_{-1}^{i,n} = -D_1(W_{i-1}^n, W_i^n) \\ B_0^{i,n} = \dfrac{\delta x_i}{\Delta^n t}\, I + D_1(W_i^n, W_{i+1}^n) - D_2(W_{i-1}^n, W_i^n) \\ B_1^{i,n} = D_2(W_i^n, W_{i+1}^n) \end{cases}$$

A classical linearization is defined via differentiation by taking:

$$D_1(W_i^n, W_j^n) = \frac{\partial \Phi_{ij}}{\partial W_i}(W^n) \quad \text{and} \quad D_2(W_i^n, W_j^n) = \frac{\partial \Phi_{ij}}{\partial W_j}(W^n)$$

Nevertheless, it is not always possible nor convenient to exactly compute the Jacobian matrices $\dfrac{\partial \Phi_{ij}}{\partial W_i}$ and $\dfrac{\partial \Phi_{ij}}{\partial W_j}$. In fact, it is not unusual to have some lack of differentiability of the numerical flux functions; it is the case, in particular, for both the Roe and the Rusanov schemes.

A Jacobian-free linearization for the Roe scheme was previously derived in [3, 14], which only exploits the algebraic properties of the Roe matrix and, therefore, does not depend on the specific equation of state. This approach is characterized by:

$$\begin{cases} D_1(W_i^n, W_j^n) = \tilde{J}^+(W_i^n, W_j^n) \\ D_2(W_i^n, W_j^n) = \tilde{J}^-(W_i^n, W_j^n) \end{cases} \quad \text{with } \tilde{J}^{\pm} = \frac{1}{2}\left(\tilde{J} \pm |\tilde{J}|\right)$$

However, due to its particular construction, this approach can be used only for the Roe scheme.

Alternatively, a classical linearization of type (17) consists in applying a first-order Taylor expansion in time but with a complete differentiation only for the centered part of the numerical flux function while the matrix Q_{ij} in the upwind part is frozen at time t^n (see, e.g., [8] for an application to the Roe scheme for Euler equations or [9] for shallow water equations). This results in the following approximation:

$$\begin{aligned} \Delta^n \Phi_{ij} \simeq & \frac{1}{2}\left(A(W_i^n)\Delta^n W_i + A(W_j^n)\Delta^n W_j\right) \\ & - \frac{1}{2} Q_{ij}^n \left(\Delta^n W_j - \Delta^n W_i\right) \end{aligned} \qquad (18)$$

in which A is the Jacobian matrix of F. Note that this approach can be used for any upwind scheme of type (7)-(8), independently of the differentiability or of the complexity in the differentiation of Q_{ij}. In particular, it can be used for both the Roe and Rusanov schemes.

Let us reinterpret this linearization by rewriting the time variation of the upwind term of Φ_{ij} as follows:

$$\Delta^n \Phi_{ij,u} = -\frac{Q_{ij}^n}{2}(\Delta^n W_j - \Delta^n W_i) - \Gamma_{ij}^{n,n+1} \qquad (19)$$

in which $\Gamma_{ij}^{n,n+1} \doteq \dfrac{\Delta^n Q_{ij}}{2}(W_j^{n+1} - W_i^{n+1})$.
The previous linearization is obtained just by neglecting the term $\Gamma_{ij}^{n,n+1}$. It is worth noting that this term can be neglected as long as that the solution is regular enough to satisfy:

$$W_j^{n+1} - W_i^{n+1} \propto O(\Delta x) \text{ and } \Delta^n Q_{ij} \propto O(\Delta t) \qquad (20)$$

Even if the assumption (20) is in general a reasonable one, there are situations of practical interest in which it is not satisfied. Indeed, if a discontinuity is present the magnitude of the term $W_j^{n+1} - W_i^{n+1}$ can be large independently of the size of Δx. Moreover, the term $\Delta^n Q_{ij}$ can also be large. This can happen, in particular, in presence of huge variations of the flow velocity or when the speed of sound has a stiff change in magnitude. The latter is a typical situation in presence of cavitation. Thus, a more complete linearization is proposed below for the case of the Rusanov scheme by estimating $\Gamma_{ij}^{n,n+1}$, neglected in the approximation (18). Note that fully linearized formulations for the classical Euler equations have been proposed in [20] for different upwind schemes.

Let us first notice that, the terms of Q_{ij} can be written as a composite function of two variables, a and u, as follows:

$$q_k = q_k\left(u(W_i(t), W_j(t)), a(W_i(t), W_j(t))\right) \qquad (21)$$

where $q_k = \lambda_{ij}$, λ_{ij} defined by (12) or (13), or alternatively for the case with preconditioning, $q_k = \lambda_{ij}\, d_k(M)$ (d_k given by (14)-(15)).

Then, through differentiation of (21), by neglecting terms of higher order and after some mathematical developments (see

[18] for more details), the following approximation of the previously neglected term is obtained:

$$\Gamma_{ij}^{n,n+1} \simeq \frac{1}{2} K_{ij} \Delta^n W_i - \frac{1}{2} K_{ji} \Delta^n W_j \tag{22}$$

in which the generic element of K_{ij} is defined by the following expression:

$$\left(K_{ij}\right)_{km} = \left(\frac{\partial q_k}{\partial u} \frac{\partial u}{\partial W_{i,m}} + \frac{\partial q_k}{\partial a} \frac{\partial a}{\partial W_{i,m}} \right) \left(W_{j,k}^n - W_{i,k}^n \right) \tag{23}$$

in which $W_{i,m}$ denotes the m-th element of the vector W_i. By putting everything together, the following more complete approximation of the time variation of the numerical flux function is obtained:

$$\begin{aligned} \Delta^n \Phi_{ij} \simeq & \frac{1}{2} \left(A(W_i^n) + Q_{ij}^n - K_{ij} \right) \Delta^n W_i \\ & + \frac{1}{2} \left(A(W_j^n) - Q_{ij}^n + K_{ji} \right) \Delta^n W_j \end{aligned} \tag{24}$$

Note that if K_{ij} is a null matrix, (24) reduces to (18).

Let us now make some simplifications based on physical considerations related to the particular kind of applications of interest in this study. Excepting when the flow is highly supersonic, we have that the flow derivatives of u are far smaller than the ones of a. Indeed, due to the particular equation of state under consideration (the barotropic cavitating one), when a transition from vapor to liquid occurs, this leads to a step-like change of the speed of sound of a few order of magnitudes. Consequently, it seems reasonable to neglect the variation in u in computing K_{ij} in (23), and then, to approximate the variation of the matrix Q_{ij} only through the variation in a. Under this assumption and using the fact that a only depends on the density, i.e. $a = a(\rho_i, \rho_j)$, the matrix K_{ij} previously defined in (23) reduces here to:

$$K_{ij} = \begin{pmatrix} \partial_{\rho_i} q_1 \left(\rho_j^n - \rho_i^n \right) & 0 & 0 \\ \partial_{\rho_i} q_2 \left((\rho u)_j^n - (\rho u)_i^n \right) & 0 & 0 \\ \partial_{\rho_i} q_3 \left((\rho \xi)_j^n - (\rho \xi)_i^n \right) & 0 & 0 \end{pmatrix} \tag{25}$$

in which $\partial_{\rho_i} q_k$ represents the partial derivative of q_k with respect to ρ_i, but considering only the variation in a, i.e.:

$$\partial_{\rho_i} q_k = \frac{\partial \chi_k}{\partial \rho_i} \quad \text{where} \quad \chi_k = \chi_k(\rho_i, \rho_j) = q_k \left(u, a(\rho_i, \rho_j) \right)$$

These partial derivatives are numerically computed here through centered finite differences.

Second-order accurate linearized implicit time advancing The following space and time second-order accurate implicit formulation is obtained considering the MUSCL technique for space as previously defined and a second-order backward differentiation formula in time:

$$\begin{aligned} \delta x_i \frac{3W_i^{n+1} - 4W_i^n + W_i^{n-1}}{2\Delta t} + \Delta^n \Phi_{i+\frac{1}{2}} - \Delta^n \Phi_{i-\frac{1}{2}} = \\ - \left(\Phi_{i+\frac{1}{2}}^n - \Phi_{i-\frac{1}{2}}^n \right) \end{aligned} \tag{26}$$

where $\Phi_{i\pm\frac{1}{2}} = \Phi(W_{i\pm\frac{1}{2}}^-, W_{i\pm\frac{1}{2}}^+)$ are the second-order accurate numerical fluxes computed as previously described. Similarly to the 1st-order case, a linearization of $\Delta^n \Phi_{i\pm\frac{1}{2}}$ must be carried out in order to avoid the solution of a nonlinear system at each time step. However, the linearization for the second-order accurate fluxes and the solution of the resulting linear system implies significant computational costs and memory requirements. Thus, a defect-correction technique [21] is used here, which consists in iteratively solving simpler problems obtained, here, just considering the same linearization as used for the 1st-order scheme. The defect-correction iterations write as:

$$\begin{cases} \mathcal{W}^0 = W^n \\ \mathcal{B}_{-1}^{i,s} \Delta^s \mathcal{W}_{i-1} + \mathcal{B}_0^{i,s} \Delta^s \mathcal{W}_i + \mathcal{B}_1^{i,s} \Delta^s \mathcal{W}_{i+1} = \mathcal{S}_i^s \quad s = 0, \cdots, m-1 \\ W^{n+1} = \mathcal{W}^m \end{cases}$$

in which:

$$\begin{cases} \mathcal{B}_{-1}^{i,s} = -D_1(\mathcal{W}_{i-1}^s, \mathcal{W}_i^s) \\ \mathcal{B}_0^{i,s} = \dfrac{3\delta x_i}{2\Delta t} I + D_1(\mathcal{W}_i^s, \mathcal{W}_{i+1}^s) - D_2(\mathcal{W}_{i-1}^s, \mathcal{W}_i^s) \\ \mathcal{B}_1^{i,s} = D_2(\mathcal{W}_i^s, \mathcal{W}_{i+1}^s) \\ \mathcal{S}_i^s = -\left(\dfrac{\delta x_i}{2\Delta t} (3\mathcal{W}_i^s - 4W_i^n + W_i^{n-1}) + \Phi_{i+\frac{1}{2}}^s - \Phi_{i-\frac{1}{2}}^s \right) \end{cases}$$

D_1 and D_2 being the generic matrices of the approximation (17). m is typically chosen equal to 2. Indeed, it can be shown [3, 21] that only one defect-correction iteration is theoretically needed to reach a second-order accuracy while few additional iterations (one or two) can improve the robustness.

Extension to 3D

In 3D, starting from an unstructured tetrahedral grid, a dual finite-volume tessellation is obtained by the rule of medians: a cell C_i is built around each vertex i, and boundaries between cells are made of triangular interface facets. Each of these facets has a mid-edge, a face centroid, and a tetrahedron centroid as vertices.

The semi-discrete balance applied to cell C_i reads (not accounting for boundary contributions):

$$V_i \frac{dW_i}{dt} + \sum_{j \in \mathcal{K}(i)} \Phi_{ij} = 0 \tag{27}$$

where $W_i = (\rho_i, \rho_i u_i, \rho_i v_i, \rho_i w_i)^T$ is the semi-discrete unknown associated with C_i, V_i is the cell volume, $\mathcal{K}(i)$ represents the set of nodes joined to N_i through an edge and Φ_{ij} denotes the numerical flux crossing the boundary ∂C_{ij} shared by C_i and C_j (positive towards C_j).

Once defined $\vec{\nu}_{ij}$ as the integral over ∂C_{ij} of the outer unit normal to the cell boundary, it is possible to approximate Φ_{ij} by exploiting a 1D flux function between W_i and W_j, along the direction $\vec{\nu}_{ij}$ and the extension of the schemes previously presented is straightforward. More details on the 3D formulation can be found in [2, 16] for the formulation based on the Roe scheme.

NUMERICAL EXPERIMENTS

Barotropic 1D flows in a convergent-divergent nozzle

Inviscid flows in a quasi 1D convergent-divergent nozzle are first considered. The governing equations are the reduced 1D Euler equations (without passive scalar) with a source term, which accounts for variations of the cross-sectional area S of the nozzle. More precisely, the following system of differential equations is obtained:

$$\frac{\partial W}{\partial t} + \frac{\partial F(W)}{\partial x} = -\frac{1}{S(x)} \frac{dS}{dx} G(W)$$

with $W = (\rho, \rho u)^T$, $F(W) = \left(\rho u, \rho u^2 + p\right)^T$ and $G(W) = \left(\rho u, \rho u^2\right)^T$.

The exact steady solution has been derived in [18] for the case of a generic barotropic equation of state, i.e. (5).

A non-cavitating polytropic flow In this first test case, a fully subsonic flow, characterized by a low Mach number value (approximately 10^{-3}), is obtained by considering the following inlet conditions $\rho_\infty = 900$, $u_\infty = 0.03$ and nozzle area ratio $S_{min}/S_\infty = 0.9$ respectively. Moreover, the following polytropic law:

$$p = \kappa \rho^{\varkappa} \tag{28}$$

with $\kappa = 2$ and $\varkappa = 0.5$ is used as equation of state. Similar test cases have been used in previous works [14, 16] to investigate the behavior of the numerical solution in the low Mach number regime, and, in particular, to validate the preconditioning defined for the Roe scheme. Thus, the purpose, here, is to verify that the Rusanov scheme requires a preconditioning strategy, and successively, to validate the technique proposed in (14)-(15). Fig. 1 shows the comparison between the preconditioned and the non-preconditioned simulations, as well as between the Roe and the Rusanov schemes. It turns out that a preconditioner is actually needed and the proposed one seems effective. The two versions of the Rusanov scheme (RC and RR, i.e. using (12) and (13) respectively) provide the same steady solution which appears slightly less accurate than the one obtained using the Roe

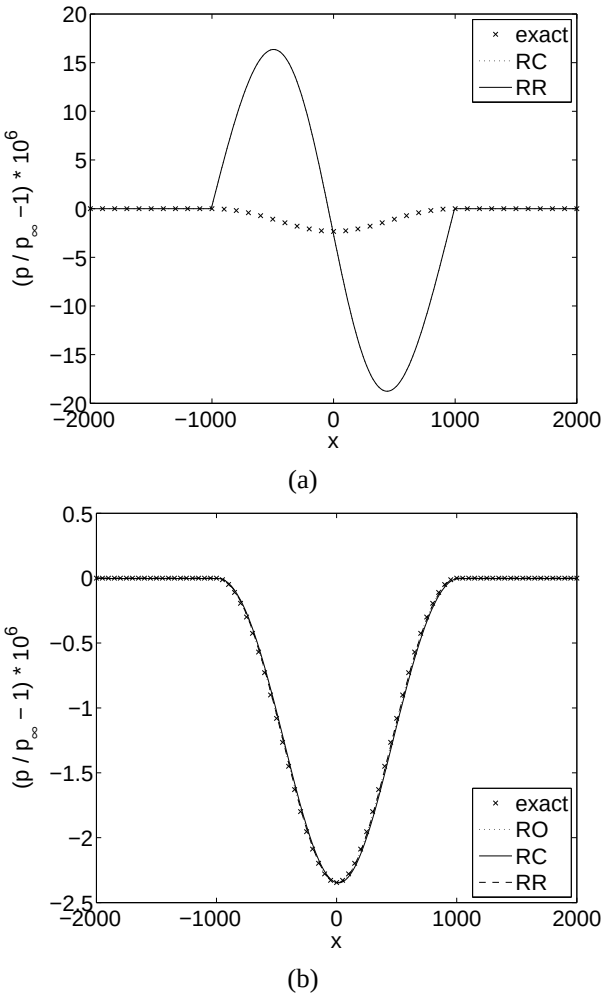

Figure 1. Comparison between Roe and Rusanov flux functions for the pressure field, $\Delta x = L/4000$: a) Without preconditioning; b) with preconditioning.

scheme. Note that, only the first-order formulations of the considered schemes have been used in the 1D simulations.

A complete cavitating 1D flow This second test case is characterized by $\rho_\infty \simeq 997.94994$, $u_\infty \simeq 1.0005$ and $S_{min}/S_\infty = 0.5$, while the equations of state (1)-(2) for cavitating flows are used by taking $T_L = 293.16$ and $\zeta = 0.1$. A subsonic/supersonic cavitating flow with a steady shock wave is then obtained. Indeed, at the inlet the flow is subsonic ($M_\infty = 1.4 \cdot 10^{-3}$) then it is accelerated through the nozzle and transitions to supersonic, then after the shock wave it becomes again subsonic. More precisely, in the convergent zone the liquid transitions to the vapor phase and at the throat the flow reaches Mach 1. Afterward the flow is expanded until Mach 14 and then, through a shock wave, the flow reverts to subsonic. This test case contains all the difficulties typically encountered in cavitating conditions: two smooth flow regions are divided by a shock wave, very high variations of Mach number values are present in the flow with both highly compressible and incompressible areas and there are liquid/vapor and vapor/liquid transitions. This test case is aimed at validating the preconditioning technique in the cavitating case as well as at evaluating the behavior of the schemes in presence of discontinuities.

It has been shown in previous studies [2, 14, 16, 10] that strong stability limitations appear when cavitation occurs for the case of a preconditioned linearized Roe formulation. Thus, by taking a fixed spatial grid ($\Delta x = L/250$), the convergence behavior has been analyzed for a large range of Δt values and different approaches. In accordance with the previous studies, the Roe scheme is constrained by a stability condition that limits the maximum CFL coefficient to a small value, here of about 0.01. The same limitation is also observed for the first Rusanov formulation, i.e. when the linearization (18) is using, even if the Rusanov scheme is known to be more robust than the Roe one. Conversely, by adopting the more complete linearization, i.e. (24)-(25), this limit is increased up to 1400. Thus, even if the unbounded time step allowed in non-cavitating conditions is not recovered, the Rusanov scheme with the complete linearization can be considered a major improvement in term of robustness, since an increase of five orders of magnitude is obtained for the CFL coefficient. These results confirm the hypothesis that the more complete linearization takes into account terms that become important when a subsonic phase transition or a shock wave (or both) are present.

Moreover, Fig. 2 shows that all the formulations based on the Rusanov flux function provide results similar in accuracy which are in rather good agreement with the exact solution. Conversely, the Roe scheme introduces an unphysical expansion shock wave and, as a consequence, the solution given by the numerical scheme is not accurate: this is the well-know problem of the entropy violation of the Roe scheme and would require an entropy fix (see, e.g., [7]).

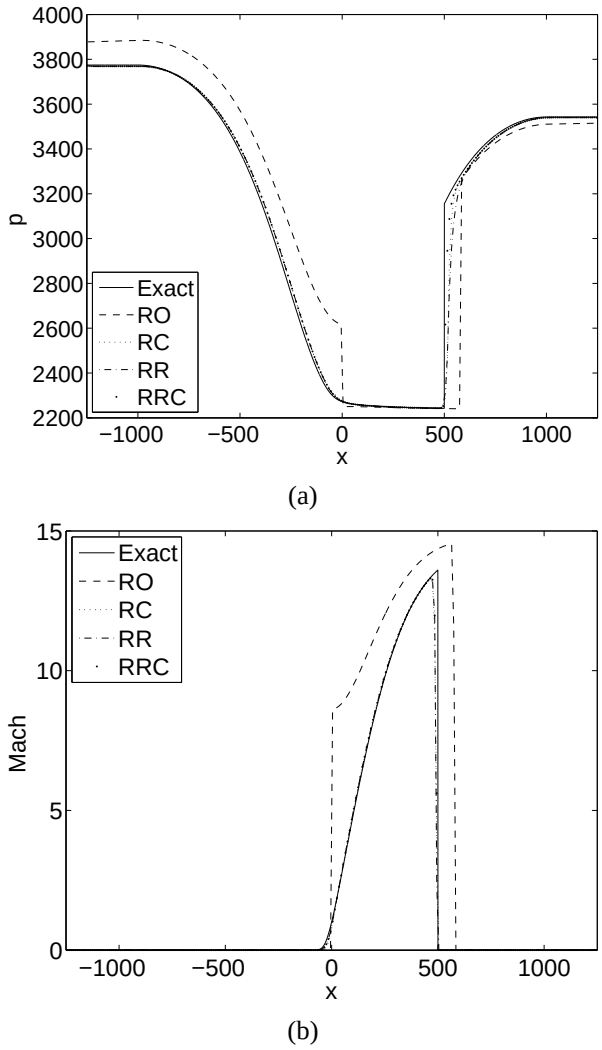

Figure 2. Comparison between Roe and Rusanov flux functions $\Delta x = L/250$: a) pressure b) Mach number.

Flow over a NACA0015 hydrofoil

The liquid flow over a NACA0015 hydrofoil in cavitating and non-cavitating conditions is considered. The hydrofoil of chord length c equal to 115 *mm* is mounted in a water tunnel at 4° incidence angle and spans the entire width of the rectangular test chamber section. The test section, which is obtained by cutting the chamber along its symmetry plane, is sketched in Fig. 3. This configuration has been considered in an experimental study in [11] for which the pressure coefficient distribution on the symmetry plane of the hydrofoil is available, together with visualizations of the attached cavitation zone. This test case was a benchmark problem considered at the conference "Mathematical and Numerical aspects of Low Mach Number Flows", Porquerolles, France, June 21-25 2004, for which a numerical study was performed with the Roe scheme (see [10]). Here, two different sets of inlet conditions are considered as summarized in Tab.

1; the first conditions (TC1) correspond to a non-cavitating case while the second ones (TC2) generate a cavitating flow.

Test case	U_∞ (m/s)	P_∞ (Pa)	T (K)	M_∞	σ_∞
TC1	3.115	59050	293.15	2.2×10^{-3}	11.71
TC2	3.115	7500	293.15	2.2×10^{-3}	1.066

Table 1. Test case inlet conditions (σ_∞ being the inlet cavitation number).

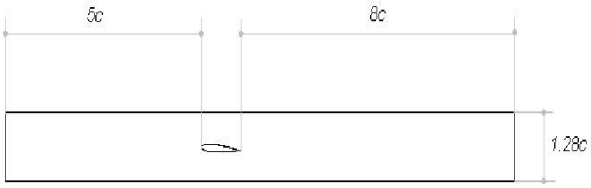

Figure 3. Sketch of the test section.

Even if the numerical discretization is fully 3D, this simulation corresponds to a 2D flow since the computation domain is an almost 2D domain, consisting in a slice of 0.1 c thickness in the spanwise direction. The grid is made of 115728 nodes; a zoom near the hydrofoil is shown in Fig. 4. Free-slip conditions have been used on the wind tunnel walls and on the hydrofoil surface. Characteristic based inflow and outflow conditions are imposed.

Results of the non-cavitating simulations

As for the 1D case, for all the considered schemes large CFL values can be used for non-cavitating flows; here, a CFL value of 200 has been chosen for the different simulations. Since this already led to very reduced computational times, a systematic analysis of the actual stability limit has not been carried out for these simulations. Actually, the initial flow for second-order simulations has been the final flow condition of the first-order computation, but this has been done only for practical purposes, i.e. to reduce the time to reach the steady solution.

The pressure coefficient distribution obtained on the hydrofoil in the different simulations is shown in Fig. 5 together with the

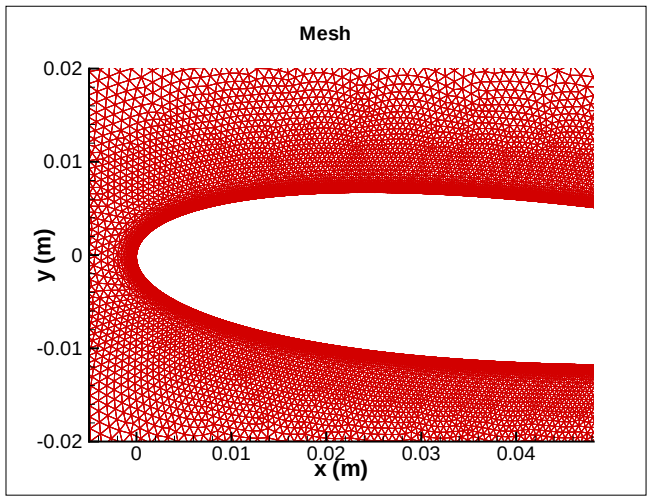

Figure 4. Zoom of the computation grid.

experimental data. It is clear that the second-order version improves the accuracy of the results for both the Roe and the Rusanov fluxes; indeed, the suction peak is correctly predicted in the 2nd-order simulations, while in the 1st-order simulation this peak is underestimated due to the excessive introduced numerical viscosity. Concerning the first-order formulation, the Rusanov scheme seems rather less accurate than the Roe one, however, for the second-order case, the two schemes furnish similar results.

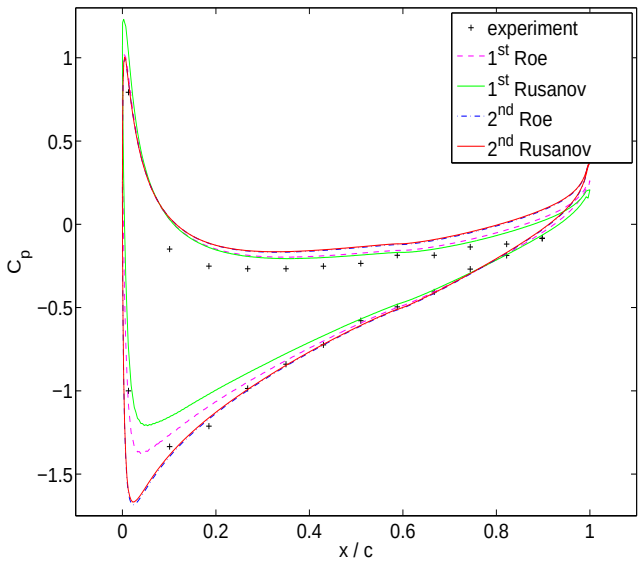

Figure 5. C_p distribution for the TC1 test case (non-cavitating flow).

Results for cavitating conditions

As previously observed for the 1D case, when cavitation occurs, the stability properties of the schemes change dramatically. For the first-order accurate formulations, the general behavior observed for the cavitating 1D flow is recovered here. Indeed, for the Roe scheme and for the Rusanov one with the first linearization (18), the CFL coefficient is limited to about 0.01, while the more complete Rusanov linearization permits to reach $CFL = 25$. The increase in the maximum allowed CFL value is, here, of more than three orders of magnitude, which is remarkable even if it is lower than that obtained in the 1D case.

Only the simulations carried out with the most efficient approach, i.e. the Rusanov one with the more complete time linearization, have been advanced in time sufficiently to obtain meaningful results. For the results given by the Roe scheme, although on a different grid, we refer to [10]. Fig. 6 shows the C_p distribution on the upper side of the hydrofoil obtained with the 1st-order accurate version of this scheme together with the relevant experimental data. The solid line is the distribution obtained at a given time step, when a generally steady condition is reached except for a small oscillation of the position of the end of the cavitation zone. First of all, note the good agreement with the experimental data obtained in both cavitating and non cavitating regions. The peak in the C_p distribution at the end of the cavitation zone is due to the previously mentioned oscillation in time of the end of this region and this peak is indeed eliminated by averaging the C_p over several time steps (dashed line). This unsteady behavior is also in agreement with the experiments, in which the length of the cavitation bubble was found to oscillate in time between $x/c = 0.4$ and $x/c = 0.46$. Conversely, it could not be observed in the Roe simulations in [10], probably because a too short time interval could be simulated due to the previously discussed limitations of the allowable time step. Fig. 7 shows the instantaneous iso-contours of the Mach number and of the cavitation number obtained in these present simulations with the Rusanov scheme. A rather large cavitation region, corresponding to negative values of the cavitation number, is present in the upper part of the hydrofoil, whose length is approximately $0.4\,c$, again in good agreement with the experimental findings. Conversely, this length was significantly underestimated in the simulations with the Roe scheme in [10], confirming that probably a steady condition was not reached in those simulations. Note also how, very large Mach number values, up to approximately 28, are reached in the cavitating region. This largely contributes to render the numerical simulation of this type of flows particularly stiff. Let us analyze now the results obtained with the 2nd-order version of the Rusanov scheme with the more complete time linearization. As for robustness, the maximum CFL value allowed in this simulation by numerical stability was 0.6. This value is is noticeably reduced with respect to the 1st-order version of the considered scheme, but it still more than one order of magnitude larger than the one found for the 1-st order Roe scheme or for the

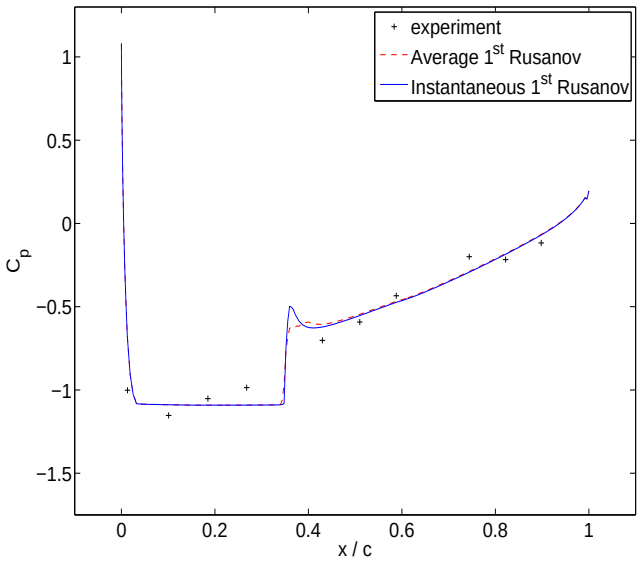

Figure 6. C_p distribution for the TC2 test case (cavitating flow).

Rusanov one with the incomplete linearization. Moreover, the sensitivity to some numerical parameters, such as the number of iterations in the defect correction approach, ad-hoc designed limiters or preconditioning of the linear system to be solved at each time step, are currently under investigation. This might give important insights on how to limit this efficiency reduction. As a consequence of the time step limitation, the 2nd-order simulation could not be advanced enough in time to reach a steady situation, but the cavitation region is still growing in time. This can be seen, for instance, in the averaged C_p distribution in Fig. 8 or in the instantaneous iso-contours of the cavitation and Mach numbers in Fig. 9 (compare with Fig. 7), in which the size of the cavitating region is smaller that in the 1st-order simulations. Except for this problem, however, Fig. 8 shows that the effects of the 2nd-order accuracy are noticeable only in a small zone near the leading edge, while in the cavitating region the C_p is almost equal to that obtained in the 1st-order simulations. The discrepancies in the rear part of the hydrofoil are again due to the lack of convergence in the 2nd-order simulations; indeed, the values of C_p in that zone have been observed to decrease in time, as the cavitation region size increases.

CONCLUSIONS

The behavior of two different numerical fluxes, namely the Roe and Rusanov schemes, has been investigated in the simulation of cavitating flows through a numerical method based on a finite-volume discretization in space and a linearized implicit time advancing. For the Rusanov scheme, two different time linearizations are proposed; in the first one the upwind part of the flux function is frozen in time, while in the second one its

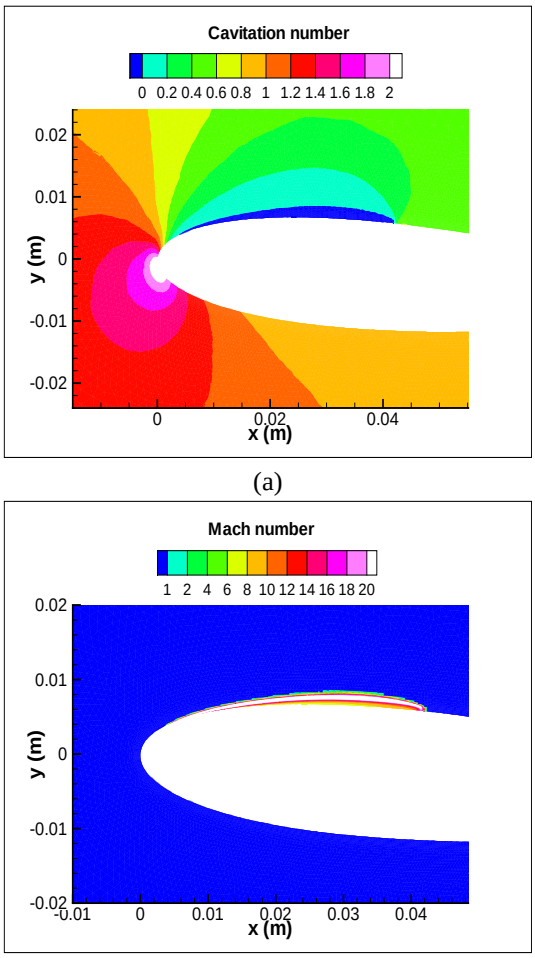

Figure 7. Cavitating conditions and 1st-order simulations: instantaneous iso-contours of the cavitation number (a) and of the Mach number (b).

time variation is taken into account, although in an approximated manner. This may be important when the speed of sound has a stiff change in magnitude, as typically occurs for homogeneous-flow models in presence of cavitation.

The different schemes and linearizations have been first appraised in the simulations of a quasi-1D flow in a convergent-divergent nozzle, both in non-cavitating and cavitating conditions. Exact solutions were available for these flows from previous works [18]. As a first-order scheme is generally more stable than the corresponding second-order one and we were mainly interested in robustness, in this first set of simulations the first-order version of the considered schemes was only used. The non-cavitating simulations show that preconditioning is needed also for the Rusanov scheme to overcome accuracy problems in the low Mach limit and validate the adopted preconditioning procedure. For non-cavitating flows a practically unbounded value of the CFL number can be used for all the schemes, while, when cavitation occurs, the Roe scheme and the Rusanov one with

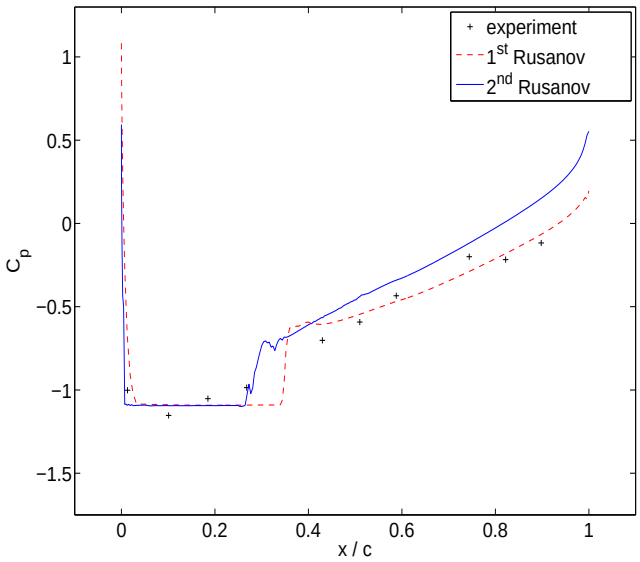

Figure 8. TC2: C_p distribution (averaged values). Comparison between first- and second-order formulations.

the first linearization suffer of stability problems which limit the maximum allowed CFL to very low values. Conversely, with the Rusanov scheme and the more complete linearization this limit is increased of five orders of magnitude. This confirms our speculation that taking into account in the linearization the time variation of the upwind part of the numerical flux is important in cavitating conditions, due to stiff changes of several order of magnitudes in the speed of sound. As for accuracy, the results obtained with the Rusanov scheme show a similar and even better accuracy agreement with the exact solutions than those given by the Roe scheme, since the latter suffers of an entropy violation problem, which should be cured by ad-hoc fix.

The different numerical formulations have then been applied to the simulation of the inviscid flow around a hydrofoil mounted in a wind tunnel both in cavitating and non-cavitating conditions. For the 1st-order version of the schemes, as previously observed for the 1D case, when cavitation occurs, the efficiency of the Roe scheme and of the Rusanov one with the incomplete linearization dramatically deteriorate and the CFL is limited to very low values. Conversely, for the Rusanov flux with the more complete time linearization, this limit is increased of more than three orders of magnitude, which is remarkable even if it is lower than that obtained in the 1D case. The obtained results are in good agreement with the experimental data, both for the pressure distribution over hydrofoil and the size and position of the cavitating region. When the 2nd-order accurate version of the Rusanov scheme with the more complete time linearization is used, the maximum reachable CFL value is only one order of magnitude larger than the one found for the 1-st order Roe scheme. However, the sensitivity to some numerical parameters in the 2nd-order formulation, such as the number of iterations in the defect

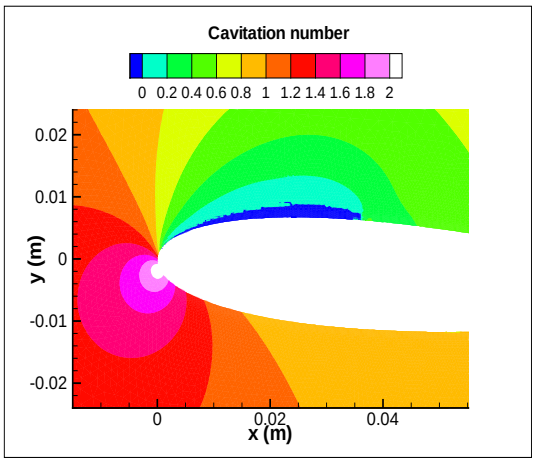

(a)

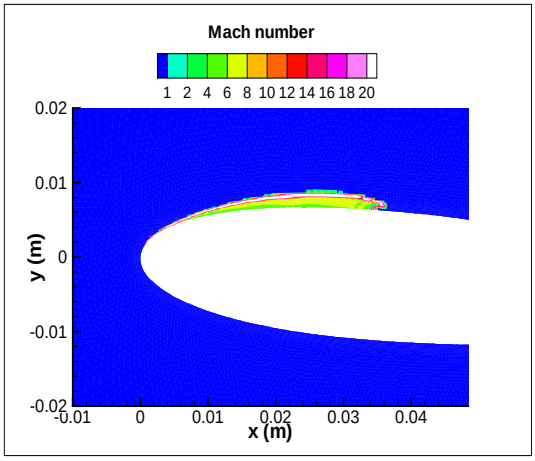

(b)

Figure 9. Cavitating conditions and 2nd-order simulations: instantaneous iso-contours of the cavitation number (a) and of the Mach number (b).

correction approach, ad-hoc designed limiters or preconditioning of the linear system to be solved at each time step, are currently under investigation. This might give important insights on possible ways how to limit this efficiency reduction. Moreover, 2nd-order accuracy is essential when dealing with viscous flows. However, in this case complex interactions between the cavitating region and the boundary layer occur, which leads to an unsteady flow behavior. In this context, the time step limitations of the 2nd-order scheme might be not so critical. Anyway, viscous simulations of the hydrofoil flow are in progress with the Rusanov scheme (properly modified to deal with contact discontinuities) together with a P1 finite-element discretization for the viscous terms, and the results will be forthcoming.

NOMENCLATURE

L length of the computational domain (for 1D studies).

CFL Courant-Friedrich-Lewy condition: $CFL = a_{\max}\dfrac{\Delta t}{\Delta x}$ in which $a_{\max}$ is the maximum speed of sound in the flow field.

RO implicit linearized Roe formulation.

RC implicit linearized Rusanov formulation using λ_{ij} from (12) and the linearization (18).

RR implicit linearized Rusanov formulation using λ_{ij} from (13) and the linearization (18).

RRC implicit linearized Rusanov formulation using λ_{ij} from (13) and the linearization (24)-(25).

C_p pressure coefficient $C_p = \dfrac{p - p_\infty}{\frac{1}{2}\rho_\infty u_\infty^2}$

σ cavitation number $\sigma = \dfrac{p - p_{sat}}{\frac{1}{2}\rho_\infty u_\infty^2}$

ACKNOWLEDGMENT

Support by ESA, under the contract No. 20081/06/NL/IA, “Scaling of Thermal Cavitation Effects on Cavitation-Induced Instabilities”, is acknowledged. The authors wish also to thank CINECA for providing the computational resources and support.

REFERENCES

[1] d’Agostino, L., Rapposelli, E., Pascarella, C. and Ciucci, A.A. 2001. ”A Modified Bubbly Isenthalpic Model for Numerical Simulation of Cavitating Flows,” *37th AIAA/ASME/SAE/ASEE Joint Propulsion Conference*, Salt Lake City, UT, USA.

[2] Sinibaldi, E., Beux, F. and Salvetti, M.V. 2006. “A numerical method for 3D barotropic flows in turbomachinery,” *Flow, Turbulence and Combustion*, 76/4, 371–381.

[3] Sinibaldi, E., Beux, F., Bilanceri, M. and Salvetti, M.V. 2008. “A second-order linearised implicit formulation for hyperbolic conservation laws, with application to barotropic flows,” *ADIA 2008-4 Report*, Pisa University.

[4] Roe, P. L. 1981. “Approximate Riemann solvers, parameter vectors, and difference schemes,” *Journal of Computational Physics*, 43, 357-372.

[5] Van Leer, B. 1979. “Towards the ultimate conservative scheme, V. A second-order sequel to Godunov’s method”, *Journal of Computational Physics*, 32, 101-136.

[6] Davis, S.F. 1988. “Simplified second-order Godunov-type methods,” *SIAM Journal of Scientific and Statistical Computing*, 9/3.

[7] Toro, E.F. 1997. *Riemann solvers and numerical methods for fluid dynamics*, Springer.

[8] Yee, H.C. 1987. “Construction of explicit and implicit symmetric TVD schemes and their applications,” *Journal of Computational Physics*, 68/1, 151.

[9] Delis, A. I., Skeels, C. P. and Ryrie, S.C. 2000. “Implicit high-resolution methods for modelling one-dimensional

open channel flow", *Journal of Hydraulic Research*, 38/5, 369–382.

[10] Beux, F., Salvetti, M.-V., Ignatyev, A., Li, D., Merkle, C. and Sinibaldi, E. 2005. "A numerical study of non-cavitating and cavitating liquid flow around a hydrofoil," *Mathematical Modelling and Numerical Analysis*, 39/3, 577-590.

[11] Cervone, A., Bramanti, C., Rapposelli, E. and d'Agostino, L. 2006. "Thermal cavitation experiments on a NACA 0015 hydrofoil," *Journal of Fluids Engineering, Transactions of the ASME*, 128/2, 326-331.

[12] Park, S.H. and Kwon, J.H. 2003. "On the dissipation mechanism of Godunov-type schemes," *Journal of Computational Physics*, 188/2, 524–542.

[13] Brennen, C.E. 1995. " ," *Cavitation and bubble dynamics*, Oxford University Press, New York.

[14] Sinibaldi, E. 2006. "Implicit preconditioned numerical schemes for the simulation of three-dimensional barotropic flows," PhD Thesis, Scuola Normale Superiore di Pisa. Series: Publications of the Scuola Normale Superiore Subseries: Theses (Scuola Normale Superiore) , Vol. 3, 2007, Approx. 235 p., Softcover.

[15] Guillard, H. and Viozat, C. 1999. "On the behaviour of upwind schemes in the low Mach number limit", *Computers & Fluids*, 28, 63-86.

[16] Salvetti, M. V., Sinibaldi, E. and Beux, F. 2007. "Towards the simulation of cavitating flows in inducers through a homogeneous barotropic flow model," *Fluid Dynamics of Cavitation and Cavitating Turbopumps*, Vol. 496 of *CISM Courses and Lectures*, SpringerWienNewYork, pp. 317–351.

[17] Li, X.-S and Gu, C.-W. 2008. "An all-speed Roe-type scheme and its asymptotic analysis of low Mach number behaviour," *Journal of Computational Physics*, 227/10, 5144–5159.

[18] Bilanceri, M., Beux, F. and Salvetti, M.V. 2008. "Investigation on numerical schemes, preconditioning and time advancing in the simulation of 1D cavitating flows," *ADIA 2008-7 Report*, Pisa University.

[19] Harten, A, Lax, P.D. and Van Leer, B. 1983. "On upstream differencing and Godunov-type schemes for hyperbolic conservation laws", *SIAM Revue*, 25, 35-61.

[20] Batten, P., Leschziner, M. A. and Goldberg, U. C. 1997. "Average-state Jacobians and implicit methods for compressible viscous and turbulent flows," *Journal of Computational Physics*, 137/1, 38–78.

[21] Martin, R. and Guillard, H. 1996. "Second-order defect-correction scheme for unsteady problems", *Computers & Fluids*, 25/1, 9-27.